

Nuclear Magnetic Resonance in Aluminum Alloys*

Yuh Fukai[†]*Department of Metallurgy and Mining Engineering and Materials Research Laboratory
University of Illinois, Urbana-Champaign, Illinois 61801*

and

Kenji Watanabe

*Department of Physics, Chuo University, Bunkyo-ku, Tokyo, Japan
(Received 6 April 1970)*

The variation of nuclear magnetic absorption intensity with solute concentration is studied in dilute alloys of aluminum. Wipe-out numbers obtained for Cu, Ag, Mg, Zn, Ga, and Si in Al are, in order, 236, 205, 122, 94, 160, and 199. An interpretation of these results in terms of the pseudopotential theory is attempted with moderate success. A systematic discrepancy is found between theory and experiments; theoretical estimates of wipe-out numbers are about 0.7 of observed values. The same theory applied to the electric field gradient on near neighbors of impurity atoms is found to give poor agreement with reported results of double-resonance experiments. It is suggested that one of the primary sources of these discrepancies is the neglect of the Bloch character of conduction electrons in calculating the screening charge distribution.

I. INTRODUCTION

The effect of alloying on the nuclear magnetic resonance of aluminum has been studied by a number of workers,¹⁻¹¹ and has been interpreted in terms of the electric quadrupole perturbation produced by impurity atoms. There are two different types of experiment; (i) a measurement of the rate of change of resonance intensity with impurity concentration,¹⁻⁵ and (ii) a measurement of the electric field gradient (EFG) on each particular shell of atoms surrounding an impurity.⁶⁻¹¹ Although the latter type of data should be of more importance eventually in establishing a microscopic picture of impurity states, the former is no less important, as it is accessible to some extent by the present state of theory, and serves therefore as a more useful guide for a better understanding of the problem.

The experiment was performed here to provide a more reliable set of intensity data to be compared with theory. There has been some doubt about the reliability of existing data because of the possible formation of small clusters of impurity atoms in the course of sample preparation. In fact, a drastic intensity change was found in Al-Ag alloys as a result of annealing at room temperature for only a few minutes.

There are also some problems on the theoretical side. Let it be accepted that the primary source of the quadrupole interaction is a long-range oscillation of the screening charge density around impurity atoms (Friedel oscillation), which varies

as $A \cos(2k_F r + \phi)/r^3$. Since the work of Kohn and Vosko¹² and of Blandin and Friedel,¹³ it has become a common practice to estimate A and ϕ in this expression by a partial-wave analysis, determining a set of phase shifts from the Friedel sum rule and observed values of residual resistivity. One might expect that this approach, based on the free-electron model, should work fairly well in aluminum because aluminum behaves like a free-electron metal in many respects. This expectation was, however, questioned in our treatment of the electrical resistivity in aluminum alloys¹⁴ (hereafter referred to as I), in which the free-electron theory was found to yield resistivity values about 0.6 times the observed ones, and this discrepancy was removed almost completely by taking the Bloch character of conduction electrons into account. In the theory presented here, we attempt to interpret experimental data in terms of the pseudopotential theory, using the same potentials that have been used in the resistivity calculation in I. Those potentials have been constructed from band-structure or Fermi-surface data and are known to give resistivity values in good agreement with observation.

Experiments performed on six impurity species Cu, Ag, Mg, Zn, Ga, and Si are described in Sec. II, followed by the description of the theory in Sec. III. A comparison between theory and experiment is discussed in some detail in Sec. IV.

II. EXPERIMENTAL

A major point of the present experiment was to

avoid a precipitation or pre-precipitation of solute atoms, which is fairly common in aluminum alloys.

Specimens were prepared from 99.999% pure aluminum and 99.99% pure alloying elements. Ingots were made by melting the constituents under high-purity argon, casting into graphite molds, and then swaging heavily. They were subsequently cold rolled into foils, about 15 μm thick and 2 cm wide. The actual composition of alloys was determined by spectroscopic analysis.¹⁵ Strips 15 cm long were then mounted on light aluminum frames, suspended in a vertical furnace filled with high-purity nitrogen, held at 550 $^{\circ}\text{C}$ for 3 h, and then quenched. In the quenching process, the foil was dropped into ethyl alcohol held at -50°C , rinsed in ether also held at -50°C , shaken vigorously to remove excessive ether, and transferred into a liquid-nitrogen reservoir. A remaining ether film was found to break off instantly. The whole quenching process was completed in 5 sec. The foils were cut into 1 \times 2-cm pieces and assembled into a sample container, leaf over leaf, with an insulating 25- μm -thick Mylar film, all in liquid-nitrogen bath. Each sample consisted of 91 pieces of foil. A sample of pure aluminum was prepared in the same way, except that it was slowly cooled after annealing, and was assembled at room temperature. A sample container was inserted snugly into an rf coil in a cryostat which had been cooled to liquid-nitrogen temperature.

The NMR spectrometer used is a twin- T Anderson-type bridge, equipped with an automatic balance control and an electronic-calibrator circuit. Derivatives of absorption lines were recorded at a fixed frequency (4 MHz) using a sinusoidal field modulation at 22 Hz. A peak-to-peak deflection of a derivative signal was calibrated against an electronic-calibrator signal, and was used as a measure of the intensity. The signal-to-noise ratio was about 15 for most concentrated alloys, and was generally better. The average was taken of nine successive runs with a sample rotated by 22.5 $^{\circ}$ each time with respect to the external magnetic field. This procedure was necessary because an orientation dependence of intensity was observed in most cases, apparently owing to rolling textures in the foils. The thickness was measured and the skin depth was calculated for each specimen in order to make a correction for the finite thickness of foils by using the result of Chapman *et al.*¹⁶ The intensity, corrected next for the number of nuclei in the sample, was normalized to that of the pure specimen. Since the effect of alloying in aluminum is known to be well described by the first-order quadrupole perturbation, which leaves $\frac{9}{35}$ of the total intensity (central line component) unaffected, we focus our attention on the rest (satel-

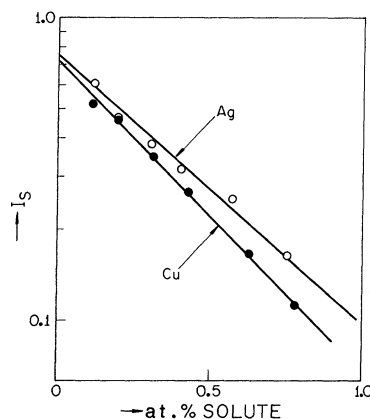


FIG. 1. Variation of satellite intensity of Al^{27} as a function of solute concentration: Cu and Ag in Al. The peak-to-peak deflection of an absorption derivative minus the central line component is taken as a measure of satellite intensity, I_s . Wipe-out numbers obtained are 236 and 205 for Cu and Ag, respectively.

lite component) and renormalize the satellite intensity to that of the pure specimen. The variation of the satellite intensity I_s with solute concentration c was fitted to an empirical formula, $I_s = (1 - c)^n$, i. e., $\ln I_s \approx -nc$, where the exponent n is a wipe-out number, which we determine from experiment.

The observed satellite intensity is plotted in Figs. 1-4 as a function of solute concentration. Note that the ordinate is a logarithmic scale. The fact that best-fit lines in these graphs do not extrapolate to unity can be largely ascribed to the effect of quenching strain; the satellite intensity of about

TABLE I. Wipe-Out number for aluminum alloys.

Impurity	Experimental		Theoretical	
	Present data	Previous data	A ^a	B ^b
Cu	236	242 ^c	153	164
Ag	205	46 ^d , 90 ^e	165	177
Mg	122	130 ^f	81	85
Zn	94	98 ^f , 100 ^g	66	69
Ga	160	...	138	149
Si	199	...	142	157
Ge	...	40 ^g , 130 ^h	176	195

^aBased on the dielectric function without exchange correction.

^bBased on the dielectric function with exchange correction.

^cReference 5.

^dReference 2.

^eReference 4.

^fReference 1.

^gReference 3.

^hReference 11.

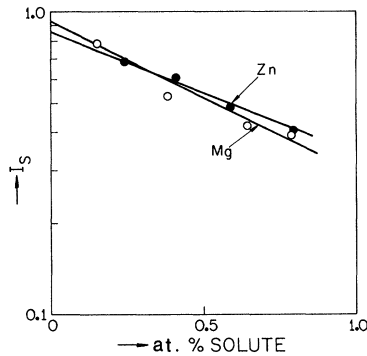


FIG. 2. Variation of satellite intensity of Al^{27} as a function of solute concentration: Mg and Zn in Al. The peak-to-peak deflection of an absorption derivative minus the central line component is taken as a measure of satellite intensity, I_s . Wipe-out numbers obtained are 122 and 94 for Mg and Zn, respectively.

0.9, observed for a pure specimen quenched in the same way as alloy specimens, comes near extrapolated values. Thus, we prefer to determine wipe-out numbers from slopes of straight lines omitting the point for the pure specimen which had been annealed before measurements. The wipe-out numbers obtained are listed in Table I, together with previously reported values.

III. THEORETICAL

It is now well established that a primary effect of alloying on the nuclear magnetic resonance of aluminum comes through the quadrupole interaction, which in turn arises mainly from the inhomogeneous (or oscillatory) distribution of screen-

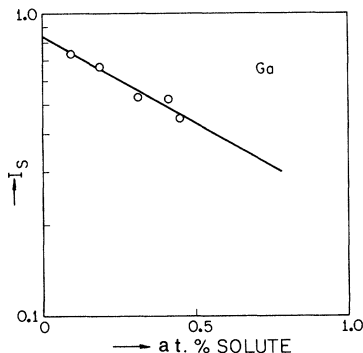


FIG. 3. Variation of satellite intensity of Al^{27} as a function of solute concentration: Ga in Al. The peak-to-peak deflection of an absorption derivative minus the central line component is taken as a measure of satellite intensity, I_s . The wipe-out number obtained is 160.

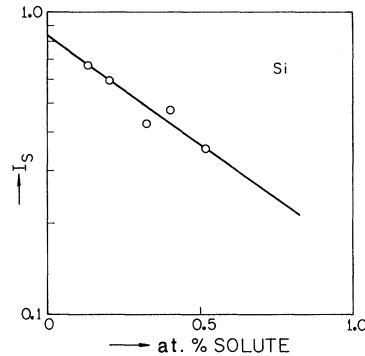


FIG. 4. Variation of satellite intensity of Al^{27} as a function of solute concentration: Si in Al. The peak-to-peak deflection of an absorption derivative minus the central line component is taken as a measure of satellite intensity, I_s . The wipe-out number obtained is 199.

ing charges around impurity atoms.

We start with the expression derived by Kohn and Vosko,¹² and Blandin and Friedel,¹³ which gives the EFG $eq(r)$ in terms of the change in charge density $\Delta\rho(r)$ introduced by an impurity atom;

$$eq(r) = (8\pi e/3)\alpha\Delta\rho(r) \quad (3.1)$$

where r is a distance from the impurity atom, and α is a constant determined by the electronic structure of the host metal and is called a core enhancement factor. The charge density $\Delta\rho(r)$ in this equation denotes only the smooth part of the screening charge density, which carries with it a rapidly varying part arising from the interaction with ion cores of host atoms. The effect of the latter is to enhance the EFG seen by the nucleus sitting at the center of the ion, and is written here in terms of the core enhancement factor. This factorization is based on the approximation that the variation of $\Delta\rho(r)$ is small over the atomic size, and is only approximately valid in actual situations.

In the following, we calculate, in order, the screening charge distribution around various impurity ions in aluminum, the core enhancement factor for aluminum, both by the pseudopotential theory, and finally the EFG and wipe-out numbers to be compared with experiment.

A. Distribution of Screening Charge around Impurity Atoms

The pseudopotential theory is used in calculating the distribution of screening charges around impurity atoms.¹⁷ It should be noted first that in pure aluminum the EFG on any aluminum nucleus vanishes because the electric charge distribution has cubic symmetry around any lattice site.

What gives rise to the nonvanishing EFG is not,

TABLE II. Core radius R (unit Å). All values except those footnoted have been obtained in Ref. 14 from the best fit to experimental points furnished by de Haas-van Alphen or optical data on pure metals.

Atom	Mg	Al	Si	Cu	Zn	Ga	Ge	Ag
R	0.732	0.610	0.522	0.93 ^a	0.683	0.535 ^b	0.506	0.99 ^a

^aEmpirical values given by N. W. Ashcroft and D. C. Langreth [Phys. Rev. **159**, 500 (1967)].

^bDetermined by interpolation.

therefore, the screening charge density around each impurity atom as a whole, but its deviation from that of an aluminum atom replaced by the impurity.

The charge density $\Delta\rho(r)$ to be used in (3.1) is then given by the pseudopotential theory as follows:

$$\Delta\rho(r) = \sum_{\vec{q}}' e^{i\vec{q} \cdot \vec{r}} \frac{q^2}{4\pi e^2} [1 - \epsilon_0(q)] \frac{\Delta w(q)}{N}, \quad (3.2)$$

where $\epsilon_0(q)$ is the dielectric function of the host metal, and $\Delta w(q)$ is a difference of the pseudopotential of the impurity atom $w_i(q)$ and that of the host atom $w_0(q)$, i. e.,

$$\Delta w(q) = w_i(q) - w_0(q). \quad (3.3)$$

The prime on the summation indicates that the $\vec{q} = 0$ term is to be omitted.

The potentials used in the present calculation are the same ones as have been used in the resistivity calculation in I. They are approximated by Ashcroft's form,¹⁸

$$w(q) = -4\pi e^2 Z \cos(qR) / q^2 \Omega_0 \epsilon_0(q), \quad (3.4)$$

where Z and R are the valence and the core radius, respectively, of the atom in question. Values of the core radius, the only parameter in the potential, have been fitted to the results of band-structure or Fermi-surface studies and are listed in

Table II. Details of the method of determining the core radius are given in I. The dielectric function in the random-phase approximation (RPA) is given as follows:

$$\epsilon_0(x) = 1 + (4\lambda^2/x^2)[f(x)/g(x)], \quad (3.5)$$

where

$$f(x) = \frac{1}{2} + \frac{4-x^2}{8x} \ln \left| \frac{2+x}{2-x} \right|, \quad (3.6)$$

and $x = q/k_F$, $\lambda^2 = 1/\pi a_0 k_F$, with a_0 the Bohr radius. Two different forms are used for $g(x)$: In one case, neglecting the exchange correction, we put

$$g(x) = 1, \quad (3.7a)$$

and in the other, including the exchange correction,

$$g(x) = 1 - \frac{\lambda^2 f(x)}{\frac{1}{2} e x^2 + 1/(1 + 0.158\lambda^2)}. \quad (3.7b)$$

Examples of the screening charge distribution calculated are shown in Figs. 5 and 6 for Mg and Si in Al. In these graphs, the quantity $\Delta\rho(r)r^3$ is plotted against r/a , where a is a lattice constant of aluminum. Also shown in the graphs is $\Delta Z(r)$, a number of screening charges contained within a sphere of radius r . Both quantities are shown for two different choices of the dielectric function. It may be seen in these graphs that the requirement for the charge neutrality is fulfilled as it should be

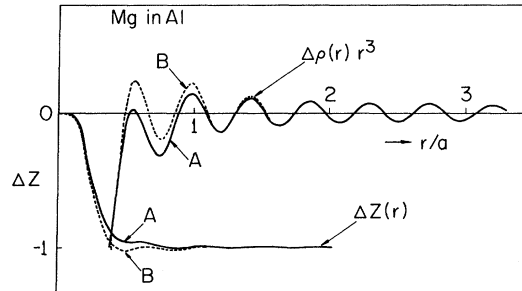


FIG. 5. Screening charge distribution around an impurity atom; Mg in Al. The screening charge density $\Delta\rho(r)$ multiplied by r^3 , and $\Delta Z(r)$, a number of screening charges contained in a sphere of radius r are shown for two different forms of the dielectric function, $\epsilon(q)$. A, solid line, $\epsilon(q)$ without exchange correction; B, dashed line, $\epsilon(q)$ with exchange correction.

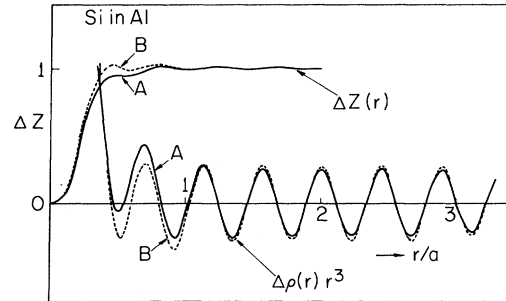


FIG. 6. Screening charge distribution around an impurity atom; Si in Al. The screening charge density $\Delta\rho(r)$ multiplied by r^3 , and $\Delta Z(r)$, a number of screening charges contained in a sphere of radius r are shown for two different forms of the dielectric function, $\epsilon(q)$. A, solid line, $\epsilon(q)$ without exchange correction; B, dashed line, $\epsilon(q)$ with exchange correction.

by virtue of the self-consistent way of constructing potentials to first order, and that the general outlook of the charge distribution fits fairly well with the asymptotic form, except that the decay of oscillation amplitude with distance is a little more rapid.

B. Core Enhancement Factor

The definition of the core enhancement factor has been given by Kohn and Vosko¹² as follows:

$$\alpha = \int d\vec{R} [\psi_{\vec{k}}^0]^2 \frac{1+\gamma(R)}{R^3} P_2(\cos\theta_{\vec{k}\vec{R}}) / \int d\vec{R} [\psi_{\vec{k}}^0]^2 \frac{1}{R^3} P_2(\cos\theta_{\vec{k}\vec{R}}) , \quad (3.8)$$

where $\psi_{\vec{k}}^0$ is a plane wave, $\psi_{\vec{k}}$ is a true wave function of conduction electrons for $|\vec{k}| = k_F$, $\gamma(R)$ is the antishielding function which takes care of small distortion of the ion core owing to quadrupole interactions, and the distance \vec{R} is measured from the aluminum nucleus in question.

In previous calculations,^{12,13} $\psi_{\vec{k}}$ has been approximated by a simple orthogonalized plane wave (OPW),

$$|\text{OPW}\rangle_{\vec{k}} = (\psi_{\vec{k}}^0 - \sum_t \phi_t \langle \phi_t | \psi_{\vec{k}}^0 \rangle) / N_{\vec{k}} , \quad (3.9)$$

where ϕ_t 's are core wave functions specified by t , and $N_{\vec{k}}$ is a normalization constant. The core enhancement factor obtained for aluminum was $\alpha = 10$.¹⁹

In the present calculation, the wave function is constructed by the pseudopotential theory, treating the array of the pseudopotential of constituent aluminum atoms as a first-order perturbation on the OPW. The expression is given as follows:

$$\psi_{\vec{k}} = |\text{OPW}\rangle_{\vec{k}} + \frac{1}{N} \sum_{\vec{q}}' \frac{w_0(q)}{E_{\vec{k}} - E_{\vec{k}+\vec{q}}} \sum_l e^{-i\vec{q} \cdot \vec{R}_l} |\text{OPW}\rangle_{\vec{k}+\vec{q}, l} , \quad (3.10)$$

where $w_0(q)$ is a pseudopotential of the host atom, the summation over \vec{q} excludes $\vec{q} = 0$, and the sum over l runs over all the lattice sites \vec{R}_l , the total number of which in the crystal is N .

The OPW's were constructed here from core wave functions calculated by Froese.²⁰ Two different forms were used for the pseudopotential of aluminum; one with an RPA dielectric function without including the exchange correction, and the other including it. The wave function (3.10) was then expanded in series of Legendre polynomials to facilitate computation of the core enhancement factor.

The core enhancement factor obtained is as follows: For the dielectric function without exchange correction, $\alpha = 22.6$, and for that with exchange

correction, $\alpha = 22.8$. The result thus proved to be quite insensitive to the choice of the dielectric function. A fact to be noticed here is that the contribution of the second term in Eq. (3.10) (screening) is equally as important as that of the first term: The first term alone gives 10.6, in agreement with the previous estimate of about 10 based on a single OPW.

C. EFG and Wipe-Out Numbers

The EFG on aluminum nuclei around impurity atoms can be obtained from Eq. (3.1) by simply substituting $\Delta\rho(r)$ evaluated at each lattice site. Results of the calculation are given in Table III for six different impurity species, together with experimental results reported.⁹ Values of the EFG on the first and second nearest neighbors to the impurity are given in units of 10^{13} cgs esu. The agreement is by no means satisfactory. The discussion of these results will be deferred to Sec. IV

In the calculation of wipe-out numbers, we adopt a method of Sagalyn *et al.*,²¹ in which the wipe-out number is written in a form

$$n = \sum_i n_i f(eq_i) , \quad (3.11)$$

where n_i is a number of atoms in shell i , and $f(eq_i)$ is a wipe-out fraction determined by the EFG

TABLE III. EFG on first and second shells from impurity atoms in aluminum (10^{13} cgs esu).

Impurity	Shell	Theoretical		Experimental ^c
		A ^a	B ^b	
Cu	1	-6.6	0.9	...
	2	2.1	3.0	...
Ag	1	-5.8	2.0	10.3
	2	2.5	3.4	2.5
Mg	1	-5.6	-2.4	8.9
	2	1.0	1.4	3.0
Zn	1	-4.5	-1.1	8.6
	2	0.7	1.1	1.7
Ga	1	3.8	4.6	1.7
	2	-0.1	-0.1	10.6
In	1	3.1
	2	16.3
Si	1	8.3	5.7	3.6
	2	-0.6	-1.0	13.2
Ge	1	9.4	7.1	2.6
	2	-0.6	-1.0	15.4

^aBased on the dielectric function without exchange correction.

^bBased on the dielectric function with exchange correction.

^cReference 9. The sign of EFG undetermined from experiments.

on that shell, eq_i . As the experiment here deals with the peak-to-peak deflection of absorption derivatives in randomly oriented crystallites, the appropriate expression for the wipe-out fraction is

$$f(eq) = \left[1 - \left(\frac{dg}{d\nu} \right)_{\max} \middle/ \left(\frac{dg_0}{d\nu} \right)_{\max} \right] \middle/ \left(1 - \frac{9}{35} \right), \quad (3.12)$$

where $(dg_0/d\nu)_{\max}$ is a maximum deflection of the absorption derivative in pure aluminum, and $(dg/d\nu)_{\max}$ is a corresponding quantity for a hypothetical sample with all the aluminum nuclei exposed to the same value of EFG, eq . The former is evaluated from the observed line shape in pure aluminum, while the latter is calculated by convolution of the frequency distribution function in a powder sample for a given value of eq , and the line-shape function in pure aluminum. The electric quadrupole moment of ^{27}Al is taken to be $Q = 0.149 \times 10^{-24} \text{ cm}^2$. The wipe-out fraction obtained is shown in Fig. 7 as a function of eq . The wipe-out numbers calculated are listed in Table I, together with experimental ones. Calculated values are in reasonable agreement with experiment, although they are consistently smaller than experiment by about 30%. These results will be discussed in some detail in Sec. IV.

IV. DISCUSSION

We attempt in this section to examine some possible defects of the theory from the over-all comparison between theoretical and experimental results.

The fact to be noted first is that the present theory yielded results reasonably good for wipe-out numbers but rather poor for the EFG on near

neighbors of impurity atoms. This implies that the theory works better in the distant region than in the near-neighbor region; the wipe-out number is a kind of average quantity determined by the EFG distribution at large distances from impurities. A little closer look reveals the following: (i) As regards wipe-out numbers, the discrepancy between theory and experiment found for six different impurity species is more systematic than random. The ratios of the observed to calculated wipe-out numbers are about 1.4 on the average. (ii) As regards the EFG on near neighbors, two distinct features are noticed. Firstly, the theory predicts the EFG on the nearest-neighbor aluminum nuclei larger than on the next-nearest-neighbor nuclei for all impurity species, whereas the experiment shows that the reverse is the case for impurity atoms with valence $Z \geq 3$. Secondly, the EFG calculated by the theory has axial symmetry on any aluminum atom as a consequence of spherically symmetric screening charge distribution assumed, whereas a definite deviation from axial symmetry was found from experiment, the asymmetry factor for Zn impurity, for example, amounting to as large as $\eta = 0.39$.⁹

We now proceed to examine some possible sources of these discrepancies. One might be tempted to ascribe them to the effect of lattice distortion which has been neglected in the present calculation. The effect, if any, should be more important in the near-neighbor region than in the distant region. This conjecture, however, seems disproved by the observation: There exists a clear correspondence between the values of EFG observed with different impurities of the same valence, although the local lattice distortion as deduced from the lattice parameter change is widely different. Certainly, the effect must be responsible, at least in part, to the observed deviation from axial symmetry, but this seems to be outweighed by something connected with the valence of impurities in determining the over-all feature of the EFG distribution.

The systematic discrepancy noted with wipe-out numbers deserves consideration. It is instructive to recall in this connection that the same kind of discrepancy was found in I for the electrical resistivity calculated by the ordinary pseudopotential theory using the same potentials that are used in the present theory. The systematic discrepancy in that case was explained nearly completely by taking the Bloch character of conduction electrons into account. The effective enhancement of the scattering matrix element caused by the Bloch character resulted in the over-all increase of the resistivity by about 60% practically irrespective of impurity species, and brought the theoretical

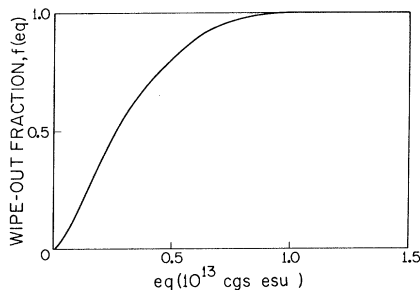


FIG. 7. Wipe-out fraction $f(eq)$ for Al^{27} in metallic aluminum. The wipe-out number for any particular kind of impurity is given in terms of $f(eq)$ by $n = \sum_i n_i f \times (eq_i)$, where n_i and eq_i are the number of atoms and EFG on the shell i surrounding an impurity atom.

estimates in good agreement with observed values. We suggest here, on this basis, that the inclusion of the Bloch character should lead to substantial improvement of the theory of EFG. The effective enhancement of the scattering matrix element noted in the resistivity calculation may be enough to enhance the EFG by the required amount of about 40%. It should also be pointed out that this effect is potentially capable of explaining the observed deviation from axial symmetry, because the crystal structure should be reflected on the screening charge distribution through the Bloch character of conduction electrons. In principle, what we have to do is to consider the dielectric response of Bloch waves instead of plane waves. This has been left out in the present paper mainly because of the amount of computational labor anticipated, and also because we preferred to present the analysis in the simplest possible form.

It may be appropriate next to examine the reliability of potentials used in this calculation. Among the problems associated with the method of constructing potentials are the choice of dielectric function and the neglect of nonlocal character of potentials. The calculation has shown that the estimates of EFG on near neighbors are greatly changed by the different choice of dielectric function, while the wipe-out numbers are only slightly affected. In any case, there is no sign of improvement as far as the EFG is concerned through the inclusion of the exchange correction in the dielectric function, although it should be more legitimate and is favored by the analysis of dispersion curves of lattice vibration. The nonlocal character of potential on the other hand was discussed in I. Suffice it to say here that this effect can be rather important for Cu, Zn, and Ag, that is, impurity atoms of lower valence with outermost *d* electrons.

Another possible question is the reliability of the estimated value of the core enhancement factor. The observed wipe-out numbers may be explained very well if we assume the core enhancement factor to be about 1.4 times larger than what we used here. Considering that this factor is not easy to estimate with high accuracy, this certainly remains a possibility as far as wipe-out numbers are concerned. In the case of near neighbors, however, the discrepancy is more or less random and cannot be ascribed to this origin. We should question rather the validity of Eq. (3.1) itself because the variation of charge density is much more rapid and larger in magnitude in this region than in the distant region. What we have to do in this case is

obvious; we have to return to the original expression for the EFG due to screening charges, namely,

$$eq(\vec{R}_n) = -2e \int d\vec{R} \Delta\rho(\vec{R}_n + \vec{R}) \frac{1+(R)}{R^3} P_2(\cos\theta_{\vec{R}_n\vec{R}}),$$

where \vec{R}_n is a position of the *n*th lattice site measured from the impurity atom, and $\Delta\rho$ is now the actual change in charge density induced by the impurity atom. Note here that the core enhancement effect is implicitly contained in the calculation of $\Delta\rho$. The total EFG is then obtained by adding to it a contribution from the electric charge on the impurity ion, $\Delta Ze(1+\gamma_\infty)/R^3$. Unfortunately, however, a literal application of the ordinary pseudopotential theory in calculating $\Delta\rho$ in this expression is not expected to yield satisfactory results. The fact that the core enhancement factor is doubled by including the screening charge distribution around an aluminum atom implies that we have to proceed at least to the second-order perturbation with respect to pseudopotentials in calculating the EFG, whereas the ordinary pseudopotential theory is based on the first-order perturbation treatment. Although this difficulty was circumvented here by taking over the result of previous workers, Eq. (3.1), it does not seem to be possible by any means to obviate this problem if a reliable calculation of the EFG on near neighbors is intended.

V. CONCLUSION

It is concluded from the comparison of pseudopotential calculations of quadrupole interactions in aluminum alloys with experiments that going beyond the free-electron theory is a necessity in the calculation of the EFG just as it is in the case of electrical resistivity (as found in I). It is also concluded that a "screening" part of the wave function of conduction electrons around a host atom plays a significant role in the core enhancement effect: The core enhancement factor of aluminum obtained here is about 23 as compared to 10, a previous estimate based on a single OPW approximation.

ACKNOWLEDGMENTS

The experimental part of this work, performed at Chuo University, was supported, in part, by a grant from the Ministry of Education, and also by a grant from Fuji Photo Film Company, to which authors are very grateful. One of the authors (Y. F.) is indebted to Professor C. A. Wert and Professor T. J. Rowland of the University of Illinois for support of the theoretical part of this work, for continual interest and stimulating discussions.

*Research supported in part by the U.S. Atomic Energy Commission under Contract No. AT(11-1)-1198.

†On leave of absence from Chuo University, Tokyo, Japan.

- ¹T. J. Rowland, *Acta Met.* **3**, 74 (1955).
- ²J. M. Titman, *J. Phys. Chem. Solids* **23**, 318 (1962).
- ³Y. Masuda, *J. Phys. Soc. Japan* **18**, 1090 (1963).
- ⁴V. S. Pavlovskaya and A. F. Edneral, *Fiz. Tverd. Tela* **6**, 2072 (1964) [*Soviet Phys. Solid State* **6**, 1635 (1965)].
- ⁵J. M. Brettel and A. J. Heeger, *Phys. Rev.* **153**, 319 (1967).
- ⁶M. B. Webb, *J. Phys. Chem. Solids* **20**, 127 (1961).
- ⁷N. Fernelius, in *Proceedings of the International Conference on Magnetic Resonance and Relaxation, Fourteenth Colloque Ampère, Ljubljana, Yugoslavia, September, 1966*, edited by R. Blinc (North-Holland, Amsterdam, 1968).
- ⁸L. E. Drain, *J. Phys. C* **1**, 1690 (1968).
- ⁹M. Minier, *Phys. Letters* **26A**, 548 (1968); *Phys. Rev.* **182**, 437 (1969).
- ¹⁰H. Launois, thesis, University of Paris (Orsay), 1969 (unpublished).
- ¹¹Cl. Berthier and P. Segransan (private communication).
- ¹²W. Kohn and S. H. Vosko, *Phys. Rev.* **119**, 912 (1960).
- ¹³A. Blandin and J. Friedel, *J. Phys. Radium* **21**, 689 (1960).
- ¹⁴Y. Fukai, *Phys. Rev.* **186**, 697 (1969).
- ¹⁵Sample preparation up to this stage was done by Tanaka Denshi Kogyo Co.
- ¹⁶A. C. Chapman, P. Rhodes, and E. F. W. Seymour, *Proc. Phys. Soc. (London)* **B70**, 345 (1957).
- ¹⁷See, for example, W. A. Harrison, *Pseudopotentials in the Theory of Metals* (Benjamin, New York, 1966).
- ¹⁸N. W. Ashcroft, *Phys. Letters* **23**, 48 (1966).
- ¹⁹A value $\alpha = 5$ given in Ref. 13 should be read as 10, because there was an error of a factor of 2 in their expression for α .
- ²⁰C. Froese, *Proc. Cambridge Phil. Soc.* **53**, 210 (1957).
- ²¹P. Sagalyn, A. Paskin, and R. J. Harrison, *Phys. Rev.* **124**, 428 (1961).

Spin-Diffusion Limitations for High-Sensitivity NMR Techniques*

P. R. Moran and D. V. Lang[†]

Physics Department, University of Wisconsin, Madison, Wisconsin 53706

(Received 16 March 1970)

The experimental sensitivity attainable in employing such high-sensitivity NMR techniques as double nuclear resonance and rotating-frame relaxation can be limited by spin-diffusion rates within the bulk detected spin system. We develop a diffusion kernel solution to the driven spin-diffusion equation and calculate the detected-system magnetization decay rate induced by a dilute concentration of pumping centers. Our results show that spin-diffusion suppression of the induced decay rate depends only upon local parameters, is independent of concentration of pumping centers, and, in all systems whose experimental study has thus far been reported, would produce at most a 10% effect. These particular conclusions apply only to the case of completely dispersed pumping centers, but the general approach can be extended to treat aggregated systems. Our description of the spin-diffusion behavior yields results in agreement with existing experimental data, but in disagreement with previous theoretical treatments.

I. INTRODUCTION

Extraordinary sensitivity for detection and study of very dilute concentrations of defect states in solids is provided by the techniques of nuclear magnetic double resonance (DNR) and of rotating-frame relaxation, $(1/T_{1\rho})$, induced by slow atomic motions. Both methods involve the same principle; an easily detected bulk nuclear resonance in the sample, which we refer to as the detected system, is adiabatically demagnetized to very low spin temperatures, and this cold detected system is brought into thermal contact with hot defect states which we refer to as pumping centers. In both cases, the

bulk detected spin system serves as an integrating detector of the energy transferred from the pumping-center defect being studied.

In the case of rotating-frame (or zero-field) relaxation experiments, spatial coordinates describing the defect are driven by the lattice dynamics and the defect couples to the bulk spins by magnetic dipole or quadrupolar interactions with a more or less broad spectrum characterized by the average jump time of the defect. Slichter and Ailion^{1,2} used this method to study the motion of free vacancies in Li metal at low temperatures; the technique was employed more recently by Kumano and Hanabusa³ and by Wagner and Moran^{4,5} to study the motions and